Geopersia 2022, 12(1): 173-189
DOI: 10.22059/GEOPE.2021.318118.648598

RESEARCH PAPER

Contamination assessment and source identification of metals and metalloids in soils around the Sari Gunay gold mine, Kurdistan Province, W Iran

Behrouz Rafiei *, Masoomeh Bakhtiari-Nejad

Department of Geology, Bu-Ali Sina University, Mahdieh St., Hamedan, Iran

Received: 29 January 2021, Revised: 08 November 2021, Accepted: 28 December 2021

Abstract
In this investigation, the level of metals and metalloids (As, Sb, Co, Cr, Hg, Pb, Zn, Ni, V, and Ti) was determined in soil samples collected from the Sari Gunay gold mine surrounding area, west of Iran. A total of 38 soil samples were taken from the area close to mine, agricultural lands, and villages. Average concentrations of heavy metals in the soil samples were as follow: Co: 13.97 mg/kg; Cr: 95.79 mg/kg; Hg: 9.03 mg/kg; Ni: 55.05 mg/kg; Pb: 163.13 mg/kg; Ti: 0.42%; V: 103.29 mg/kg; Zn: 145.42 mg/kg. The mean concentration of metalloids was 106.53 mg/kg for As and 65.68 mg/kg for Sb. The results of EF and CF indicate that soil samples were very highly polluted by As, Hg and Sb, highly polluted by Pb, moderately polluted by Zn and V, and almost unpolluted by Ti, Ni, Co, and Cr. The C_d and PLI revealed that most soil samples in the gold mine surrounding area are extremely polluted. Based on the statistical analyses, including correlation coefficient analysis, principal component analysis (PCA), and cluster analysis (CA), the main source of the elements is the orebody itself and mining activities have increased the pollution degree. Arsenic, Hg, Sb, Pb, and Zn are related to gold mineralization veins and sulfidic minerals (e.g. stibnite, realgar, orpiment, cinnabar, galena, and sphalerite), while the other metals are originated from the oxide/hydroxide of iron in the supergene alteration zone and silicate minerals existing in host rocks.

Keywords: Heavy Metal, Soil Pollution, Statistical Analysis, Sari Gunay Gold Mine, Kurdistan Province.

Introduction

Heavy metal pollution in soils has got researchers' attention today (Ruilian et al., 2008; Rafiei et al., 2010a; 2010b; Ebenebe et al., 2017; Rafiei et al., 2017; Khosravi et al., 2020). Soil is a critical environment because it can act as a scavenger agent for heavy metals produced by natural and anthropogenic activities (such as mining, industry, agriculture). However, the soil is not a passive sink of heavy metals. The polluted soils are a source of contamination for other environmental components and the food chain (Gholizadeh et al., 2015). Also, even in low concentrations, heavy metals can persist in soil for a long time (Lizárraga-Mendiola et al., 2009).

Among many anthropogenic activities, mines and mining operations are obvious sources of contamination in the surface environments and negatively impact the quality of the environment (Adriano, 1986; Donkor et al., 2005; Acosta et al., 2011; Abiya et al., 2019). The level of heavy metals and metalloids can be elevated around metalliferous mines due to mine waste dispersion into nearby soils, agricultural products, and drainage systems. The contaminated soils may pose a potential health risk to the people living around mining areas.

Many types of research are achieved on heavy metal contamination in soils, plants, waters

* Corresponding author e-mail: b_rafiei@basu.ac.ir

and sediments from metallic mines throughout the world (e.g. Fuge et al., 1989; Merrington & Alloway, 1994; Jung, 1995; Jung & Thornton, 1997; Rafiei et al., 2010a; 2010b; Mehrabi et al., 2015, Gafur et al., 2018; Karn et al., 2021).

Gold mines have been documented as a source of heavy metal contamination in soils and sediments all around the world (e.g., USA (Straskraba & Moran, 1990), South Africa (Gzik et al., 2003), Iran (Rafiei et al., 2010a; 2010b), Ghana (Armah et al., 2014), Canada (Percival et al., 2014) and Nigeria (Johnbull et al., 2019)).

Metals and metalloids associated with gold mines, including arsenic (As), cadmium (Cd), mercury (Hg), antimony (Sb), chromium (Cr), copper (Cu), lead (Pb), nickel (Ni), zinc (Zn), titanium (Ti), and vanadium (V) can be dispersed around the mines due to the weathering process of orebody and tailings (e.g. Abdul-Wahab & Marikar, 2012; Xiao et al., 2017; Mandeng et al., 2019: Okereafor et al., 2019; Adewumi & Laniyan, 2020).

The goals of this study were (1) to determine the level of contamination with heavy metals and metalloids in the soil samples around the Sari Gunay gold mine using enrichment factor (EF), contamination factor (CF), degree of contamination (C_d), and pollution load index (PLI), (2) to determine the source of the elements as well as the relationship between them, lithology and mineralogy of the study area using statistical methods.

Geological and geographical setting

The Sari Gunay gold mine is located in the northeast of Qorveh (35° 7′ 30" to 35° 14′ 00" N and 48° 1′ 30" to 48° 7′ 00" E), Kurdistan Province, in western Iran (Fig. 1). The study area consists of two main parts, Agh Dagh, and Sari Dagh, which are surrounded by several hills in the north.

The Sari Gunay gold mine is a part of the Qorveh-Takab metallogenic zone, located in the Sanandaj-Sirjan structural zone (Stöklin, 1968; Bolourchi, 1979). The oldest rocks found in this region are slate, phyllite, and Jurassic quartzite, and the youngest ones are Neogene volcanoclastic conglomerates, basaltic flows, and quaternary agglomerates (Fig. 1). The intrusive rocks of the study area are semi-deep microgranite-microgranodiorite with calc-alkaline nature and microgranular-porphyry texture (Neogene), and dacite-rhyodacite (cropped out in Agh Dagh and Sari Dagh) (Rastad et al., 2000; Niroomand et al., 2013).

These acidic to intermediate igneous rocks are mainly composed of minerals such as plagioclase, hornblende, biotite, clinopyroxene, orthopyroxene, magnetite, in smaller quantities of quartz, and sanidine (Richards et al., 2006).

Pyrite, arsenopyrite, stibnite, realgar, orpiment, galena, Sphalerite, chalcopyrite, cinnabar, tennantite, and rutile are formed by hypogene processes. Iron oxide/hydroxides (hematite and goethite) are found in the supergene alteration zone, in which sulfides are replaced by oxides, jarosite, and rare alunite (Richards et al. 2006; Ranjbarian, 2018). The Sari Gunay mine is a gold deposit hosted by a middle Miocene volcanic complex formed in epithermal veins (Rastad et al., 2000; Richards et al., 2006; Niroomand et al., 2013). There are different mineralization stages in the gold mine hydrothermal system. In the early stage, quartz-sulfide-magnetite veins were created with low-grade mineralization of copper and gold. The next stage involves creating quartz-tourmaline veins with low-grade gold. The main gold mineralization has occurred in quartz-pyrite-stibnite-realgar-orpiment veins. Arsenopyrite and locally cinnabar are also found in some veins (Richards et al., 2006).

Material and methods

Sampling

A total of 38 samples were collected from surface soils (0 to 20 cm), including mine area and

agricultural soils (Fig. 1). Sampling points were selected considering the possibility of more contamination in areas close to the mine and the rural regions. The samples were packed in polyethylene bags and sent to Bu-Ali Sina University, Hamedan, for further treatments such as physicochemical and chemical analyses.

Physicochemical analysis

Soil samples were air-dried after transferring to the laboratory for 48 hours. In order to determine the pH of samples, a mixture of soil and water was prepared in the ratio of 1 to 5 (Segura et al., 2006), and pH was measured by pH meter model 744Ω ohmmeter.

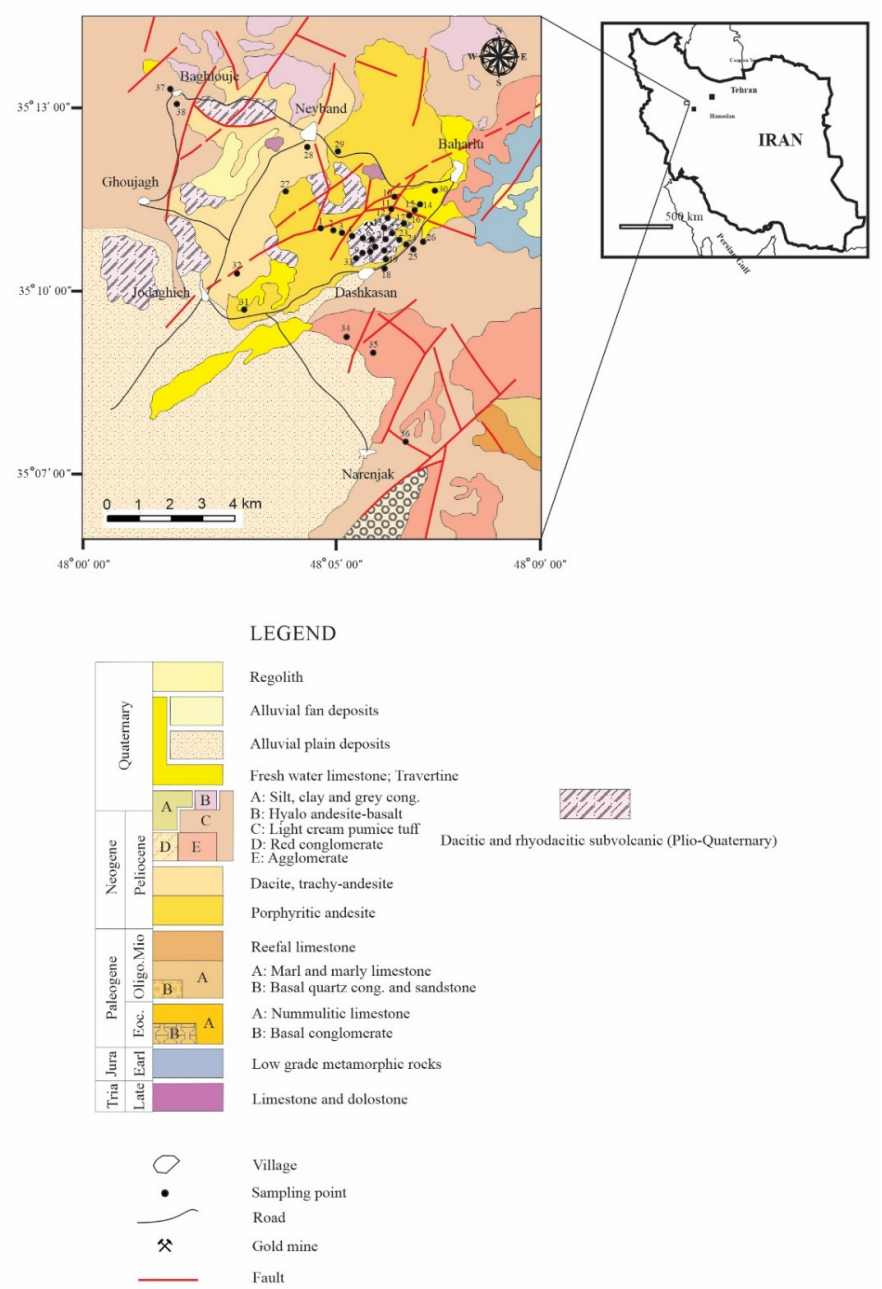

Figure 1. Simplified geological map of the study area (based on Khan Nazer, 2015), Sari Gunay mine location, and sampling sites of the investigated area

The granulometry method was used to investigate particle size distribution and texture recognition for all samples. The main part of each sample was separated from the fine grains by the wet sieving method. A column of sieves was used for the coarse-grained part (Lewis & MacConchie, 1994) where the subsample finer than 62.5 microns was tested by Fritsch A22 Compact in the sedimentological laboratory of Bu-Ali Sina University. Calcium carbonate in sediments was determined by the titration method (Carver, 1971).

Chemical analysis

The samples were passed through a 2 mm sieve and ground completely with an agate mortar for chemical analysis. Inductively coupled plasma-optical emission spectrometry (ICP-OES) was employed to determine the total concentration of elements in the samples. The soil samples were completely acid-digested with $HCl–HNO_3–HClO_4$. The cold vapor atomic absorption spectroscopy (AAS) method was used to measure mercury. These analyses were performed in the ALS Chemex Laboratory, Canada.

Contamination assessment

Enrichment factor (EF), contamination factor (CF), contamination degree (C_d) proposed by Håkanson (1980), and pollution load index (PLI) proposed by Tomlinson et al. (1980) were used to determine metal pollution in soil samples. These methods are the most common environmental pollution indices used for single and integrated elements assessments (Caeiro et al., 2005; Hou et al., 2013).

The enrichment factor (EF) is utilized to differentiate between the metals originating from anthropogenic activities and those from natural sources and assess the degree of human influences. This index is based on normalizing a given element against a reference one (Liang et al., 2017). A reference element is usually a conservative metal, such as Al, Fe, Mg, Mn, Sc, Ti (Hernandez et al., 2003; Mishra et al., 2004). In the present research, Sc was chosen as the reference element, and EF was calculated as follow:

$$EF = (C_m/C_{Sc})_{sample} / (C_m/C_{Sc})_{reference} \quad (1)$$

where, C_m is the concentration of the examined element, and C_{Sc} is the concentration of the Sc. In this equation, $(C_m/C_{Sc})_{sample}$ shows the ratio of the element and Sc concentrations in the sample and $(C_m/C_{Sc})_{reference}$ indicates their ratio in the background. To determine the degree of contamination and enrichment, five contamination categories were recognized (Sutherland, 2000): (a) deficiency to minimal enrichment (if $EF < 2$), (b) moderate enrichment (if $2 \leq EF < 5$), (c) significant enrichment (if $5 \leq EF < 20$), (d) very high enrichment (if $20 \leq EF < 40$), and (e) extremely high enrichment (if $EF > 40$).

The contamination factor (CF) is a single-metal index and calculated by the ratio of the average concentration of a metal in the soil sample (C_m) to the same metal in the background (C_{bk}):

$$CF=C_m/C_{bk} \quad (2)$$

C_{bk} in this study is the concentration of the studied metal in the Upper Continental Crust (UCC) suggested by Rudnick & Gao (2003). The background values of metals (C_{bk}) were considered as 4.8, 17.3, 92, 0.05, 47, 17, 0.4, 3100, 53 and 67 mg/kg for As, Co, Cr, Hg, Ni, Pb, Sb, Ti, V, and Zn, respectively. For this index, four classes of contamination were suggested by Håkanson (1980): (a) low contamination factor (if $CF < 1$), (b) moderate contamination factor (if $1 \leq CF < 3$), (c) considerable contamination factor (if $3 \leq CF < 6$), and (d) very high contamination factor (if $CF \geq 6$).

The contamination degree (C_d) is an integrated pollution index and defined as the sum of all CF in a particular sample and is divided into four classes (Håkanson, 1980): (a) low degree of

contamination (Cd < 8), (b) moderate degree of contamination (8 ≤ Cd < 16), (c) considerable degree of contamination (16 ≤ Cd < 32), and (d) very high degree of contamination (Cd ≥ 32). This index is calculated as follow:

$C_d = \sum_1^n CF$ (3)

The pollution load index (PLI), proposed by Tomlinson et al. (1980), is another integrated pollution index that comparatively determines each sample's heavy metal pollution level. This index is a geometrical average of CFs in a sampling site, and it is calculated by using the following equation:

$PLI = \sqrt[n]{CF_1 \times CF_2 \times \ldots \times CF_n}$ (4)

where, n is the number of metals, and CF is the contamination factor of each pollutant. The PLI value is classified into four groups (Wang et al., 2010): (a) no pollution (if PLI < 1), (b) moderate pollution (if 1 ≤ PLI < 2), (c) heavy pollution (2 ≤ PLI < 3), and (d) extreme pollution (PLI ≥ 3).

Statistical analysis

All data gathered here were subjected to process using Statistical Package for Social Sciences (SPSS) version 21 and Minitab 2020. Bivariate correlation, cluster analysis (CA), and principal component analysis (PCA) were carried out to interpret potential sources of heavy metals and metalloids in the soil samples of the study area.

The Bivariate correlation (Pearson correlation coefficient) measures the strength of the relationship between two variables (elements). Cluster analysis (CA) was performed to classify elements of different sources based on their chemical properties similarities. A dendrogram was constructed to assess the consistency of the clusters formed, in which correlations among elements are readily observed. Principal component analysis (PCA) was used to reduce data (Loska & Wiechuya, 2003) and to investigate the source of elements and the extent of metal pollution (Dragovic et al., 2008). PCA is also employed to analyze the relationship among the observed variables. The CA is complementary to PCA.

Results and discussion

Physicochemical properties of soil samples

The texture, pH value, carbonate content of soil samples are shown in Table 1. The soil textures range from muddy sand to sandy mud and silty sand to sandy silt. The samples were classified as muddy sand (two samples), silty sand (three samples), sandy mud (twenty-three samples), and sandy silt (ten samples) according to Folk (1974) textural classification (Fig. 2). Therefore, about sixty-seven percent of samples are composed of fine-grained sediments (sandy mud and sandy silt). The pH values vary from 7.15 to 7.75 (Table 1), which shows low alkaline nature. The carbonate content varies between 0.75 to 14.37 % (mean 3.40%), indicating low $CaCO_3$ in the soil samples.

Heavy metal concentration

The total concentration of As, Sb, Co, Cr, Fe, Hg, Pb, Zn, Ni, V, Ti, and S in the soil samples is presented in Table 1. The concentrations of As in the soil samples ranged from 18 to 485 mg/kg (mean 106.53 ± 91 mg/kg), and the arsenic content of 39% of samples is more than the mean value, markedly higher than its concentration in soils around the world. The overall average value of total As for soils varies from 5.0 to 6.83 mg/kg (Kabata-Pendias, 2011). High concentrations of As in the soil samples are found in the study area, particularly near the sulfide

orebody, as shown by Rafiei et al. (2010a). Concentrations of Sb ranged from 5 to 640, with an average of 65.68 ± 119 mg/kg, and 23.5% of samples show Sb level higher than the mean value. The presence of high Sb content close to the mine is also attributed to orebody and mining activities. Cobalt concentrations varied from 4 to 23 mg/kg. The mean value for Co in surface soil samples is 13.97 ± 4 mg/kg. About 58% of the samples show concentration levels higher than the mean value.

Table 1. Heavy metals and metalloids concentrations (mg/kg) and physicochemical properties of the soil samples around the Sari Gunay gold mine

Sample	Al	As	Co	Cr	Fe	Hg	Ni	Pb	S	Sb	Ti	V	Zn	pH	$CaCO_3$ %	Sand %	Silt %	Clay %
1	8.54	32	15	50	5.79	0.03	23	81	0.04	5	0.38	134	183	7.75	1.32	55.22	32.03	12.75
2	8.74	207	20	150	5.72	1.6	67	60	0.02	86	0.44	126	126	7.29	0.99	26.96	40.05	32.99
3	7.74	43	17	123	4.46	0.31	95	40	0.04	5	0.48	116	105	7.30	14.37	32.38	50.94	16.68
4	8.05	115	21	109	4.74	0.3	69	55	0.02	9	0.47	126	124	7.27	3.67	37.82	35.64	26.54
5	7.08	80	18	121	3.97	1.18	92	117	0.05	52	0.41	113	98	7.25	2.55	47.64	30.24	22.12
6	6.67	485	7	51	2.32	100	33	117	0.49	640	0.3	92	87	7.26	0.97	20.51	37.72	41.77
7	7.71	329	11	88	4.19	5.75	48	545	0.43	318	0.43	96	97	7.65	2.43	24.57	36.83	38.60
8	7.48	114	7	84	3.97	5.48	45	139	0.72	24	0.38	80	64	7.26	2.33	42.84	34.76	22.40
9	8.64	71	7	84	3.26	0.71	32	57	0.11	11	0.37	99	87	7.26	3.52	53.90	29.72	16.38
10	7.15	58	16	130	4.07	0.22	84	42	0.04	71	0.44	117	104	7.29	14.00	34.12	46.83	19.05
11	8.21	131	16	151	5.04	0.26	67	74	0.02	250	0.46	124	127	7.31	1.86	47.59	30.06	22.35
12	8.68	81	18	159	5.62	0.56	73	76	0.03	28	0.48	134	122	7.31	2.61	45.96	34.69	19.35
13	8.21	137	15	125	4.23	1.78	73	249	0.1	96	0.49	109	105	7.53	0.97	45.36	34.60	20.04
14	9.03	153	17	85	5.01	100	51	371	0.06	254	0.4	106	267	7.30	1.61	28.71	40.75	30.54
15	9.23	49	12	91	4.7	0.81	52	158	0.03	33	0.41	11	171	7.35	2.50	42.15	37.79	20.06
16	8.92	153	11	94	3.71	0.5	47	830	0.11	43	0.41	91	95	7.61	0.75	27.71	44.07	28.22
17	10.05	55	4	47	4.86	0.18	31	236	0.17	11	0.23	66	181	7.30	2.55	53.24	32.76	14.00
18	8.91	75	14	80	5.25	2.53	49	121	0.05	20	0.43	114	311	7.21	5.95	43.62	32.96	23.42
19	9.03	104	13	78	4.54	0.67	50	161	0.05	27	0.46	114	232	7.62	3.32	42.61	28.67	28.72
20	7.55	203	10	78	3.45	1.43	50	191	0.04	51	0.32	96	137	7.31	2.79	47.91	24.37	27.72
21	6.92	122	14	87	4	4.78	52	681	0.06	68	0.39	96	220	7.29	3.44	29.27	45.37	25.36
22	7.02	154	11	105	3.37	2.63	62	106	0.15	91	0.39	97	88	7.23	3.35	37.41	37.99	24.60
23	7.98	109	13	105	4.15	14.8	65	185	0.12	51	0.43	110	144	7.23	2.11	44.81	32.39	22.80
24	9.03	112	23	126	4.84	0.27	62	123	0.04	24	0.51	137	190	7.33	2.11	51.11	26.32	22.57
25	9.15	161	13	79	4.32	0.41	51	205	0.05	27	0.32	98	274	7.25	3.89	47.77	29.92	22.31
26	7.75	56	15	134	4.04	0.14	51	166	0.02	13	0.39	105	165	7.34	1.54	33.60	43.75	22.65
27	8.01	67	16	93	4.35	0.2	62	280	0.02	30	0.43	104	231	7.27	5.69	44.28	36.46	19.26
28	7.72	44	14	86	4.02	0.03	61	53	0.02	12	0.44	101	117	7.45	5.09	39.38	47.14	13.48
29	6.87	64	11	60	3.19	0.07	40	61	0.02	28	0.37	83	82	7.22	3.81	32.88	51.75	15.37
30	7.49	99	8	63	2.73	1.18	29	271	0.04	31	0.35	86	275	7.56	7.66	24.22	53.27	22.51
31	8.24	23	13	68	4.03	0.06	47	54	0.02	7	0.4	100	103	7.61	2.97	44.09	35.73	20.18
32	7.03	193	18	80	4.08	94	57	73	0.03	39	0.41	99	141	7.56	5.61	42.12	37.44	20.44
33	8.11	37	17	114	4.25	0.03	79	30	0.02	6	0.47	107	102	7.15	1.86	25.70	56.68	17.62
34	7.07	18	16	122	3.93	0.01	65	26	0.01	5	0.46	103	77	7.20	1.75	44.04	40.63	15.33
35	7.83	43	17	114	4.67	0.03	66	29	0.02	6	0.5	114	97	7.51	1.68	41.22	40.53	18.25
36	8.02	30	11	52	4.26	0.1	29	68	0.02	14	0.42	86	210	7.22	1.75	34.10	51.74	14.16
37	8.43	20	18	97	4.49	0.02	46	39	0.01	5	0.49	117	99	7.25	1.93	57.68	31.66	10.66
38	7.57	21	14	77	4.6	0.03	37	29	0.02	5	0.48	118	88	7.21	1.80	47.99	37.62	14.39
Min	6.67	18.00	4.00	47.00	2.32	0.01	23.00	26.00	0.01	5.00	0.23	11.00	64.00	7.15	0.75	20.51	24.37	10.66
Max	10.05	485.00	23.00	159.00	5.79	100.00	95.00	830.00	0.72	640.00	0.51	137.00	311.00	7.75	14.37	57.68	56.68	41.77
Mean	**8.05**	**106.53**	**13.97**	**95.79**	**4.27**	**9.03**	**55.05**	**163.13**	**0.09**	**65.68**	**0.42**	**103.29**	**145.42**	**7.35**	**3.40**	**40.07**	**38.21**	**21.73**
Median	8.02	80.50	14.00	89.50	4.24	0.46	51.50	111.50	0.04	27.50	0.43	104.50	123.00	7.30	2.53	42.38	37.14	21.28
SD	0.80	91.07	4.15	29.14	0.75	26.54	17.28	178.56	0.15	119.48	0.06	21.93	65.23	0.15	3.00	9.56	7.90	6.79

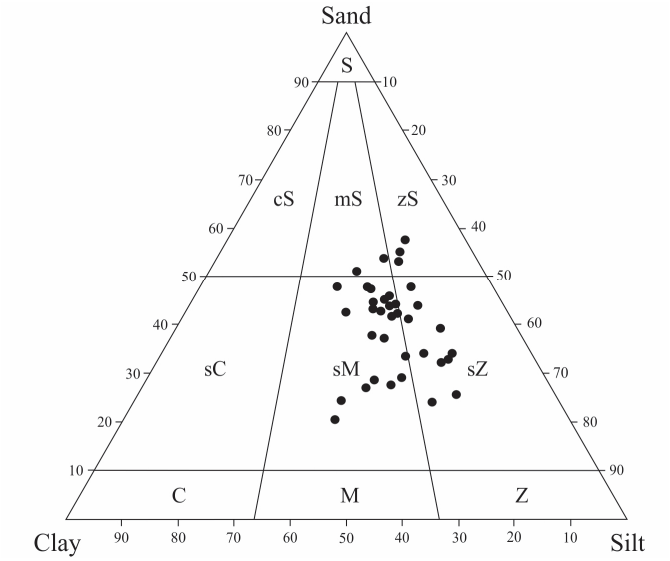

Figure 2. Textural classification of the studied soil samples based on Folk (1974). (S = sand, s = sandy; Z = silt, z = silty; M = mud, m = muddy; C = clay, c= clayey)

Chrome concentrations ranged from 47 to 159 mg/kg with an average and median of 95.79 ± 29 and 90 mg/kg, respectively, and 42% of the soil samples have Cr content higher than the mean value. Iron concentrations in the studied samples ranged between 2.32% and 5.79%. It is believed that Fe is mainly found as oxides and hydroxides in soils. The mean value of Fe is 4.27%, and near 45% of the samples indicate a higher concentration than the mean value.

Mercury concentrations ranged from 0.01 to more than 100 mg/kg (average 9.03 ± 26.54 mg/kg). The measured concentration of Hg is drastically increased toward the mine. The median value for Hg is 0.46 mg/kg. About 10% of the analyzed samples show concentration levels higher than the average value. Three soil samples 6, 14, and 32 show the highest Hg concentration (Table 1).

Concentrations of Pb and Zn ranged from 26-830 (mean 163.13 ± 178) and 64-311 (mean 145.42 ± 65) mg/kg, respectively. The highest concentrations of both metals were measured in the mining area. Close to 32% and 34% of soil samples have Pb and Zn concentrations above the mean values, respectively. Increasing lead and zinc levels are attributed to the occurrence and disintegration of galena (PbS) and sphalerite (ZnS) in the orebody.

The concentrations ranged between 23- 95 mg/kg (mean 55.05 ± 17 mg/kg), 11- 137 mg/kg (mean 103.29 ± 22 mg/kg) and 0.23 – 0.51% (mean 0.42 ± 0.06%) for Ni, V, and Ti, respectively. Based on the results presented in Table 1, about 45% of samples for Ni, 53% for V, and 50% for Ti show higher concentration levels than their average values. The highest Ni, V, and Ti levels are measured in the samples near the mining area.

The high concentrations of studied elements, especially in the samples near mine and orebody, indicate that the Sari Gunay gold mine and mining operations resulted in an extensive distribution of metals and metalloids around the mining site.

Assessment of soil Contamination

Enrichment factor (EF) is one of the most commonly used indices for pollution assessment. The EF near 1 indicates natural and geogenic origin, whereas EF values greater than 1.5 can show anthropogenic sources (Sutherland et al., 2000). Although some natural sources result in high EF in soils and sediments (such as sulfidic mines including chalcophile elements (Hg, Pb, Zn) and elements such as Fe, As, Sb, Co, and Ni), the high EF value does not entirely represent

anthropogenic origin. The results of EFs are displayed in figure 3a, b and Table 2, which shows the distribution of each element's EF. Due to vertical scale differences, the EFs of studied elements were plotted in two separated diagrams.

Table 2. Contamination assessment of the soil samples around the Sari Gunay gold mine using single-element (enrichment factor (EF) and contamination factor (CF)) and integrated-pollution (contamination degree (Cd) and pollution load index (PLI)) indices

Sample	As		Co		Cr		Cu		Hg		Ni		Pb		Sb		Ti		V		Zn			
No.	EF	CF	EF	CF	EF	CF	EF	CF	EF	CF	EF	CF	EF	CF	EF	CF	EF	CF	EF	CF	EF	CF	Cd	PLI
1	6.2	6.7	0.8	0.9	0.5	0.5	0.9	1.0	0.6	0.6	0.5	0.5	4.4	4.8	11.7	12.5	1.1	1.2	2.4	2.5	2.5	2.7	32.9	1.8
2	35.5	43.1	1.0	1.2	1.3	1.6	1.1	1.3	26.4	32.0	1.2	1.4	2.9	3.5	177.1	215.0	1.2	1.4	2.0	2.4	1.5	1.9	303.5	5.3
3	8.4	9.0	0.9	1.0	1.2	1.3	1.2	1.3	5.8	6.2	1.9	2.0	2.2	2.4	11.7	12.5	1.4	1.5	2.0	2.2	1.5	1.6	39.7	2.7
4	21.0	24.0	1.1	1.2	1.0	1.2	1.2	1.3	5.3	6.0	1.3	1.5	2.8	3.2	19.7	22.5	1.3	1.5	2.1	2.4	1.6	1.9	65.3	3.3
5	16.7	16.7	1.0	1.0	1.3	1.3	1.2	1.2	23.6	23.6	2.0	2.0	6.9	6.9	130.0	130.0	1.3	1.3	2.1	2.1	1.5	1.5	186.4	4.6
6	128.6	101.0	0.5	0.4	0.7	0.6	1.7	1.3	2545.5	2000.0	0.9	0.7	8.8	6.9	2036.4	1600.0	1.2	1.0	2.2	1.7	1.7	1.3	3713.6	7.7
7	96.0	68.5	0.9	0.6	1.3	1.0	1.7	1.2	161.0	115.0	1.4	1.0	44.9	32.1	1113.0	795.0	1.9	1.4	2.5	1.8	2.0	1.4	1017.9	7.3
8	23.8	23.8	0.4	0.4	0.9	0.9	0.9	0.9	109.6	109.6	1.0	1.0	8.2	8.2	60.0	60.0	1.2	1.2	1.5	1.5	1.0	1.0	207.5	3.9
9	18.8	14.8	0.5	0.4	1.2	0.9	0.7	0.6	18.1	14.2	0.9	0.7	4.3	3.4	35.0	27.5	1.5	1.2	2.4	1.9	1.7	1.3	66.2	2.6
10	12.1	12.1	0.9	0.9	1.4	1.4	1.3	1.3	4.4	4.4	1.8	1.8	2.5	2.5	177.5	177.5	1.4	1.4	2.2	2.2	1.6	1.6	205.8	3.5
11	25.5	27.3	0.9	0.9	1.5	1.6	1.2	1.3	4.9	5.2	1.3	1.4	4.1	4.4	583.3	625.0	1.4	1.5	2.2	2.3	1.8	1.9	671.6	4.7
12	13.9	16.9	0.9	1.0	1.4	1.7	1.1	1.3	9.2	11.2	1.3	1.6	3.7	4.5	57.6	70.0	1.3	1.5	2.1	2.5	1.5	1.8	112.8	4.0
13	25.0	28.5	0.8	0.9	1.2	1.4	1.0	1.2	31.2	35.6	1.4	1.6	12.8	14.6	210.0	240.0	1.4	1.6	1.8	2.1	1.4	1.6	327.8	5.7
14	34.3	31.9	1.1	1.0	1.0	0.9	1.3	1.3	2153.8	2000.0	1.2	1.1	23.5	21.8	683.8	635.0	1.4	1.3	2.2	2.0	4.3	4.0	2699.0	9.9
15	11.9	10.2	0.8	0.7	1.2	1.0	1.1	1.0	18.9	16.2	1.3	1.1	10.8	9.3	96.3	82.5	1.5	1.3	0.2	0.2	3.0	2.6	125.1	3.0
16	29.8	31.9	0.6	0.6	1.0	1.0	0.8	0.9	9.3	10.0	0.9	1.0	45.6	48.8	100.3	107.5	1.2	1.3	1.6	1.7	1.3	1.4	205.3	4.5
17	11.5	11.5	0.2	0.2	0.5	0.5	0.6	0.6	3.6	3.6	0.7	0.7	13.9	13.9	27.5	27.5	0.7	0.7	1.2	1.2	2.7	2.7	62.5	2.2
18	16.8	15.6	0.9	0.8	0.9	0.9	0.9	0.9	54.5	50.6	1.1	1.0	7.7	7.1	53.8	50.0	1.5	1.4	2.3	2.2	5.0	4.6	134.2	4.4
19	25.3	21.7	0.9	0.8	1.0	0.8	0.9	0.8	15.6	13.4	1.2	1.1	11.0	9.5	78.8	67.5	1.7	1.5	2.5	2.2	4.0	3.5	121.8	4.1
20	53.8	42.3	0.7	0.6	1.1	0.8	1.1	0.9	36.4	28.6	1.4	1.1	14.3	11.2	162.3	127.5	1.3	1.0	2.3	1.8	2.6	2.0	217.0	4.5
21	32.3	25.4	1.0	0.8	1.2	0.9	1.5	1.2	121.7	95.6	1.4	1.1	51.0	40.1	216.4	170.0	1.6	1.3	2.3	1.8	4.2	3.3	340.3	6.3
22	37.4	32.1	0.7	0.6	1.3	1.1	1.2	1.0	61.4	52.6	1.5	1.3	7.3	6.2	265.4	227.5	1.5	1.3	2.1	1.8	1.5	1.3	325.9	4.8
23	24.5	22.7	0.8	0.8	1.2	1.1	1.3	1.2	318.8	296.0	1.5	1.4	11.7	10.9	137.3	127.5	1.5	1.4	2.2	2.1	2.3	2.1	466.0	6.1
24	21.8	23.3	1.2	1.3	1.3	1.4	0.8	0.9	5.0	5.4	1.2	1.3	6.8	7.2	56.0	60.0	1.5	1.6	2.4	2.6	2.6	2.8	107.1	4.2
25	42.7	33.5	1.0	0.8	1.1	0.9	2.0	1.6	10.4	8.2	1.4	1.1	15.3	12.1	85.9	67.5	1.3	1.0	2.4	1.8	5.2	4.1	131.0	4.1
26	12.6	11.7	0.9	0.9	1.6	1.5	0.9	0.9	3.0	2.8	1.2	1.1	10.5	9.8	35.0	32.5	1.4	1.3	2.1	2.0	2.7	2.5	65.8	3.1
27	16.3	14.0	1.1	0.9	1.2	1.0	1.3	1.1	4.7	4.0	1.5	1.3	19.2	16.5	87.5	75.0	1.6	1.4	2.3	2.0	4.0	3.4	119.5	3.9
28	11.7	9.2	1.0	0.8	1.2	0.9	1.0	0.8	0.8	0.6	1.7	1.3	4.0	3.1	38.2	30.0	1.8	1.4	2.4	1.9	2.2	1.7	51.0	2.2
29	20.7	13.3	1.0	0.6	1.0	0.7	0.9	0.6	2.2	1.4	1.3	0.9	5.6	3.6	108.9	70.0	1.9	1.2	2.4	1.6	1.9	1.2	94.4	2.3
30	26.3	20.6	0.6	0.5	0.9	0.7	0.8	0.6	30.0	23.6	0.8	0.6	20.3	15.9	98.6	77.5	1.4	1.1	2.1	1.6	5.2	4.1	146.3	3.9
31	6.1	4.8	1.0	0.8	0.9	0.7	1.0	0.8	1.5	1.2	1.3	1.0	4.0	3.2	22.3	17.5	1.6	1.3	2.4	1.9	2.0	1.5	33.9	1.9
32	51.2	40.2	1.3	1.0	1.1	0.9	1.1	0.9	2392.7	1880.0	1.5	1.2	5.5	4.3	124.1	97.5	1.7	1.3	2.4	1.9	2.7	2.1	2030.4	6.7
33	9.0	7.7	1.1	1.0	1.4	1.2	1.3	1.1	0.7	0.6	2.0	1.7	2.1	1.8	17.5	15.0	1.8	1.5	2.4	2.0	1.8	1.5	34.0	2.0
34	4.0	3.8	1.0	0.9	1.4	1.3	0.8	0.8	0.2	0.2	1.5	1.4	1.6	1.5	13.5	12.5	1.6	1.5	2.1	1.9	1.2	1.1	26.2	1.6
35	9.0	9.0	1.0	1.0	1.2	1.2	1.1	1.1	0.6	0.6	1.4	1.4	1.7	1.7	15.0	15.0	1.6	1.6	2.2	2.2	1.4	1.4	35.1	2.0
36	8.8	6.3	0.9	0.6	0.8	0.6	1.0	0.7	2.8	2.0	0.9	0.6	5.6	4.0	49.0	35.0	1.9	1.4	2.3	1.6	4.4	3.1	55.2	2.2
37	4.5	4.2	1.1	1.0	1.1	1.1	0.9	0.9	0.4	0.4	1.1	1.0	2.5	2.3	13.5	12.5	1.7	1.6	2.4	2.2	1.6	1.5	27.7	1.7
38	4.1	4.4	0.8	0.8	0.8	0.8	0.7	0.8	0.6	0.6	0.7	0.8	1.6	1.7	11.7	12.5	1.4	1.5	2.1	2.2	1.2	1.3	26.7	1.6
Min	4.0	3.8	0.2	0.2	0.5	0.5	0.6	0.6	0.2	0.2	0.5	0.5	1.6	1.5	11.7	12.5	0.7	0.7	0.2	0.2	1.0	1.0	26.2	1.6
Max	128.6	101.0	1.3	1.3	1.6	1.7	2.0	1.6	2545.5	2000.0	2.0	2.0	51.0	48.8	2036.4	1600.0	1.9	1.6	2.5	2.6	5.2	4.6	3713.6	9.9
Mean	**25.2**	**22.2**	**0.9**	**0.8**	**1.1**	**1.0**	**1.1**	**1.0**	**215.7**	**180.6**	**1.3**	**1.2**	**10.8**	**9.6**	**190.0**	**164.2**	**1.5**	**1.3**	**2.1**	**1.9**	**2.4**	**2.2**	**385.1**	**4.0**
Median	19.8	16.8	0.9	0.8	1.2	1.0	1.1	1.0	9.3	9.1	1.3	1.1	6.8	6.6	82.3	68.8	1.5	1.4	2.2	2.0	1.9	1.8	123.4	3.9

Mercury (EF ranges from 0.2 to 2545.5 with an average of 215.7) and Sb (EF ranges from 11.7 to 2036.4 with an average of 190) have mean EFs higher than 40, indicating extremely high enrichment in soil samples. Arsenic has an average EF of about 25.2, which shows very high enrichment. The average EF of Pb is 10.8 and is classified as significant enrichment. The EFs' ranges for Zn (1–5.2) and V (0.2–2.5) are low, indicating moderate enrichment, while Ti (0.7–1.9), Ni (0.5-2), Cr (0.5-1.6) and Co (0.2-1.3) show deficiency to minimal enrichment.

The mean EFs decrease in the order of Hg > Sb > As > Pb > Zn > V > Ti > Ni > Cr > Co. The soil samples were taken from adjacent to the orebody, and the active mine area exhibits the greatest EFs for studied elements, especially Hg, Sb, As, and Pb. With average EFs higher than 10, these elements might be originated from both geogenic and anthropogenic sources. Natural physical weathering processes and mining activities can also disperse contaminant metals and metalloids around the mining area.

Contamination categories percentage based on EF values of metals and metalloids is presented in figure 4a. About 66% of soil samples have EF values higher than 40 for Sb, indicating the study area is extremely high enriched for antimony. The percent of this category for Hg, As, and Pb is 24%, 13%, and 8%, respectively. All samples show deficiency to minimal enrichment for Cr, Co, and Ti.

The distribution of each element's CF is shown in the figures. 3c, 3d, and Table 2. Antimony (CF ranges from 12.5 to 1600), As (3.8-101), Hg (0.2-2000), and Pb (1.5-48.5) have mean CFs higher than 6, Showing a very high contamination factor. The percentage of contamination

classes based on CF values of Sb, As, Hg and Pb is 100%, 89.5%, 58%, and 52% of total soil samples (Fig. 4b). The CF values of Zn ranges from 1 to 4.6; 21% of samples are classified as considerable contamination factor, and 79% are classified as moderate contamination factor. Titanium (0.7-1.6) and V (0.2-2.6) have an average of CF values 1.3 and 1.9, respectively, indicating moderate contamination factor. Ninety-seven percent of soil samples are moderately contaminated by these heavy metals. Nickel (0.2-2), Cr (0.5-1.7) and Co (0.2-1.3) show the least contamination factor in the study area. About 79% of samples for Ni, 53% for Cr and 29% for Co represent moderate contamination factors. The mean CFs decrease in the order of Hg (180.6) > Sb (164.2) > As (22.2) > Pb (9.6) > Zn (2.2) > V (1.9) > Ti (1.3) > Ni (1.2) > Cr (1.0) > Co (0.8), that shows the same trend as EF. The soil samples` C_d and PLI (integrated pollution indices) are presented in figure 3e and Table 2.

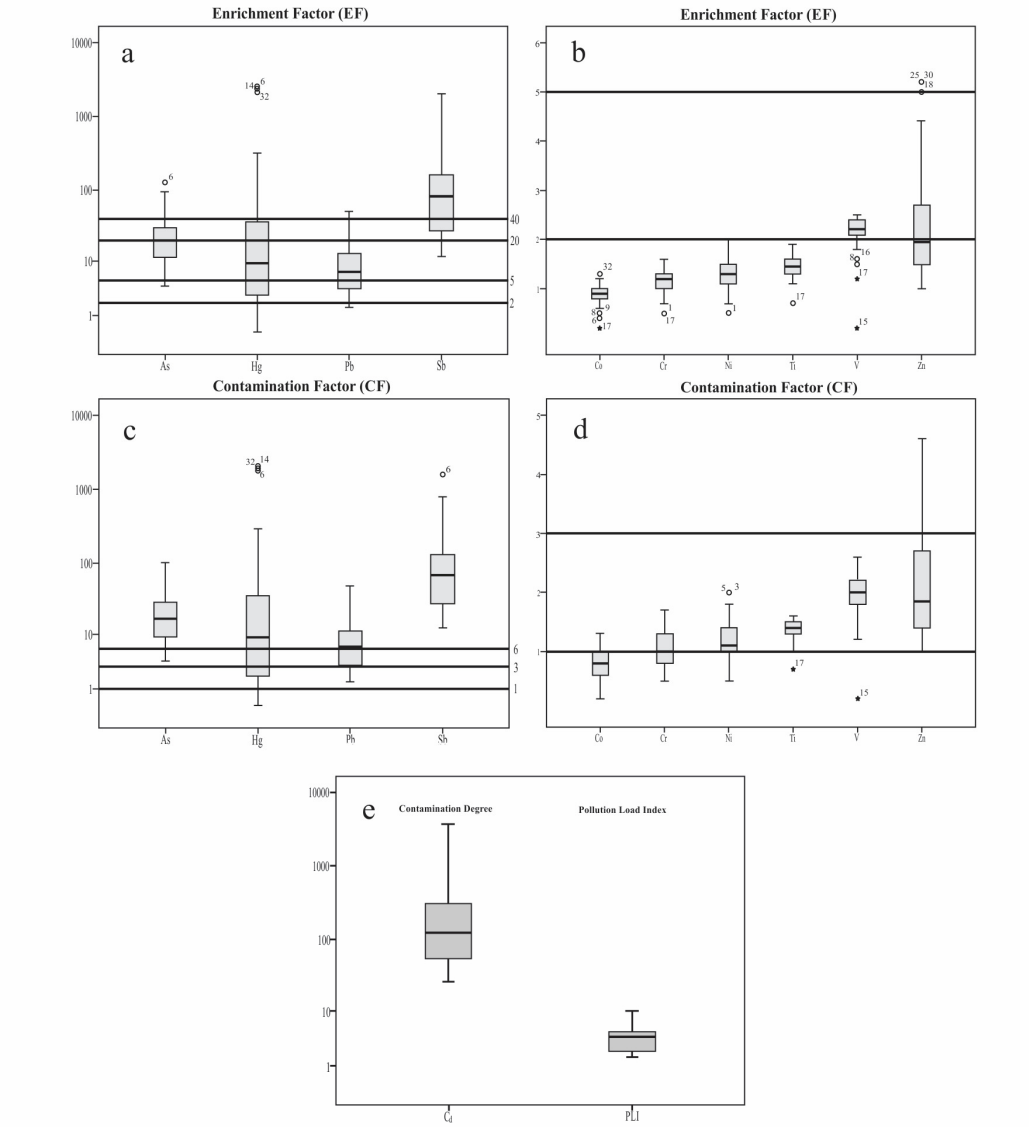

Figure 3. Box-plot of (a and b) enrichment factor (EF) (c and d) contamination factor (CF), and (e) contamination degree (C_d) and pollution load index (PLI), for some potentially toxic metals and metalloids studied in the soil samples. The EFs and CFs were plotted in two separate diagrams due to differences in the vertical axis. The median value of C_d shows very high contamination for the study area. Circles (o) show outliers in the data with corresponding sample numbers. Vertical lines show reference lines for EF and CF classifications

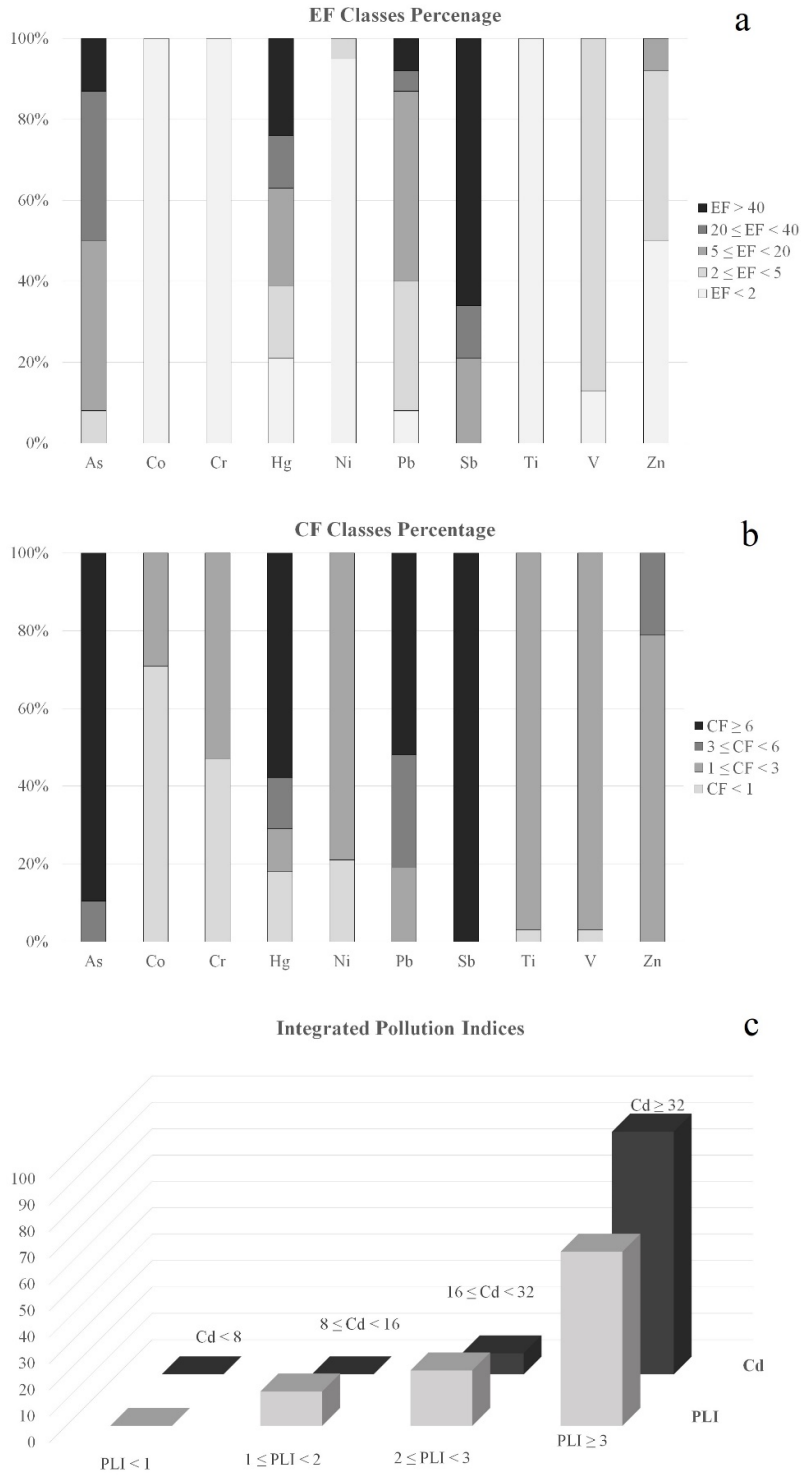

Figure 4. (a) Enrichment factor class distribution for each element in the study area. Antimony is significant to extremely high enriched in all samples. (b) Contamination factor class distribution for each element in the study area. All samples show very high CF for Sb. (c) Integrated pollution indices (C_d and PLI) in the soil samples of the study area

Contamination degree and PLI range from 26.2 to 3713.6 (mean 385.1) and 1.6 to 9.9 (mean 4.0), respectively. Based on C_d, near 92% of soil samples indicate a very high degree of contamination, and on PLI, about 66% of samples show extreme pollution (Fig. 4c). The

greatest values of C_d and PLI are observed in the soil samples adjacent to the mining site (Fig. 1 and Table 2).

Statistical Analysis

To evaluate the impact of the Sari Gunay gold mine and mining activities on the accumulation of some heavy metals and metalloids in the surrounding area of the mine, trace element concentrations in the soil samples were measured. Pollution indices showed high-level contamination for As, Sb, Hg, and Pb and medium to low-level contamination for Zn, V, Ti, Ni, Cr, and Co in the study area. The source of metals and metalloids is related to the geology and lithology of the mine area. Statistical methods were used to establish a relationship between the distribution of elements and their origin.

Pearson's correlation coefficient of elements in soil samples around the Sari Gunay gold mine is summarized in Table 3. Bivariate correlation showed that there is a strong and positive correlation between As and Hg (r=0.585), As and S (r=0.566), As and Sb (r=0.851), As and Pb (r=0.330), and a negative correlation between As and Fe (r=-0.338) and As and Ti (r=-0.331). The other strong and positive correlations are observed between Ti and Co (r=0.755), Ti and Cr (0.630), Ti and Fe (r=0.414), Ti and Ni (r=0.561), Ti and V (r=0.519). The significant positive correlation among elements in each group indicates that these elements are of a common source. The significant negative correlation between elements existing in the two separate groups shows their different origin and occurrence.

Iron, Co, Ni, As, and Sb are all chalcophile, but they can act differently in the earth's crust. Iron, Co and Ni act as chalcophile and lithophile, As and Sb as chalcophile elements. Titanium, V, and Cr elements are also lithophile metals.

Cluster analysis (CA) for potentially toxic elements in the soil samples showed that the studied elements are divided into two main clusters (Fig. 5a). The first cluster consists of As-Sb-Hg-S-Pb-Zn that is divided into two sub-clusters of 1) As-Sb-Hg-S, and 2) Pb-Zn. The second cluster, including Ti, Co, Ni, Cr, Fe, and V, can also be divided into two sub-clusters of 1) Ti-Co-Ni-Cr, and 2) Fe-V based on the cluster weight and similarities. The cluster shows that the elements are highly correlated with each other and have an identical origin.

Principal component analysis (PCA) was also applied to find metal sources in the soil samples (Table 4).

Table 3. Pearson's correlation coefficient matrix of the studied elements' concentrations

	Al	As	Co	Cr	Fe	Hg	Ni	S	Sb	Ti	V	Zn	Pb
Al	1												
As	-0.215	1											
Co	0.023	-0.22	1										
Cr	-0.014	-0.108	**0.655****	1									
Fe	**0.603****	-0.338*	**0.556****	**0.356***	1								
Hg	-0.185	**0.585****	-0.023	-0.242	-0.196	1							
Ni	-0.176	-0.12	**0.640****	**0.792****	0.208	-0.137	1						
S	-0.192	**0.566****	-0.530**	-0.242	-0.317	0.262	-0.242	1					
Sb	-0.237	**0.851****	-0.212	-0.092	-0.292	**0.635****	-0.117	**0.515****	1				
Ti	-0.029	-0.331*	**0.755****	**0.630****	**0.414****	-0.24	**0.561****	-0.335*	-0.243	1			
V	-0.054	-0.047	**0.635****	**0.457****	**0.385***	-0.064	**0.350***	-0.255	-0.044	**0.519****	1		
Zn	**0.433****	-0.063	0.008	-0.286	0.256	0.091	-0.272	-0.279	-0.099	-0.215	-0.052	1	
Pb	0.113	**0.330***	-0.245	-0.152	-0.149	0.071	-0.182	0.212	0.202	-0.227	-0.237	0.246	1

** Correlation is significant at the 0.01 level (2-tailed).

* Correlation is significant at the 0.05 level (2-tailed).

Table 4. Rotated component matrix for data of Sari Gunay gold mine (PCA loadings > 0.3 are indicated in bold)

Rotated Component Matrix[a]			
	Component		
	1	2	3
Co	**.903**	-.105	.258
Cr	**.841**	-.099	-.220
Ti	**.805**	-.252	-.043
Ni	**.783**	-.093	-.262
V	**.723**	.039	.164
As	-.094	**.922**	-.148
Sb	-.047	**.912**	-.162
Hg	-.044	**.784**	.145
S	-.352	**.528**	-.471
Pb	-.278	**.335**	.216
Zn	-.203	.032	**.885**
Fe	**.508**	-.234	**.515**

Extraction Method: Principal Component Analysis.
Rotation Method: Varimax with Kaiser Normalization.
a. Rotation converged in 6 iterations.

It shows that the elements are grouped into three components. These components (PC1, PC2, and PC3) show 69% of the total variance. PC1 includes 32% of total variability and has a high loading on Ti, Co, Cr, Ni, V, and Fe, indicating a similar source for these elements. PC2 accounts for 24% of the total variance and has positive loading on As, Sb, Hg, S, and Pb. PC3 with 13% of total variance has high loading on Zn and Fe elements. A PCA loadings plot is presented in figures 5b, c, and the relationships among the elements are readily observed. As shown in figures 5b, c, Zn and Fe are separated by a considerable distance in the PCA loading plot, suggesting that the two elements are poorly correlated (Table 3) and have different sources.

Source of the metals and metalloids

The statistical analyses showed that the elements (metals, metalloids, and sulfur) are classified into closely related groups and their source rocks. Bivariate correlation (Table 3) revealed that metals in soil samples are originated from similar geogenic and/or anthropogenic sources, particularly mine and mining activities. The strong positive correlation between elements indicates the same source for them. Arsenic shows a significant and positive correlation with Sb, Hg, Pb, and S. The strong negative correlation of As with Fe and Ti indicates different origins for these elements. It means there should be at least two distinct source rock types for the studied elements. The significant and positive correlation between Fe and Al, an element that originates from silicates, shows the existence of Fe in silicate minerals like micas and clay minerals in the soil samples. Also, Fe is positively correlated with Ti, V, Cr, and Co, indicating a similar source for these elements.

Based on cluster analysis, two groups of elements are observed. The As-Sb-Hg-S-Pb-Zn group is notably different from another group and divided into two subgroups: As-Sb-Hg-S and Pb-Zn. All elements existing in group As-Sb-Hg-S-Pb-Zn are chalcophile and tend to form sulfidic minerals. Stibnite, realgar, orpiment, cinnabar, galena, and sphalerite are the main minerals formed in the veins in the orebody and host rocks. Although two subgroups include sulfide minerals, they occurred in two different veins formed in different mineralization phases.

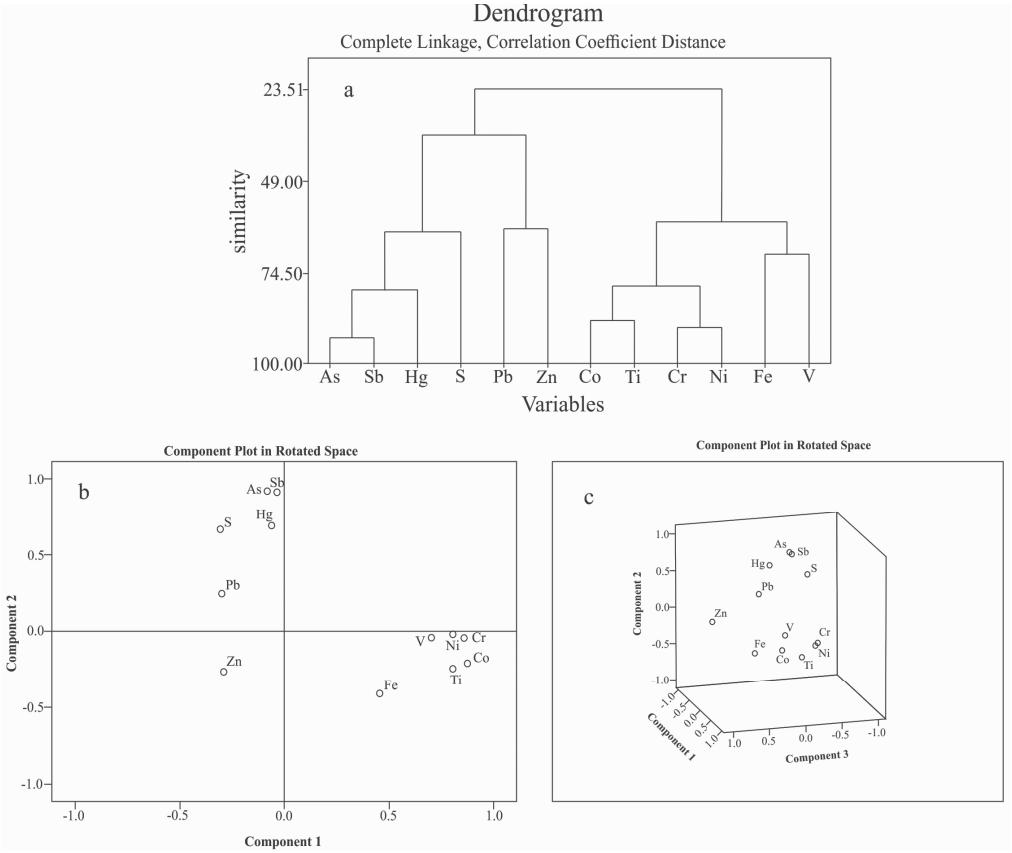

Figure 5. (a) Hierarchical dendrogram for 12 elements. Two main clusters are distinguished on this diagram, and PCA results in the 2D (b) and 3D (c) spaces (PC1 vs. PC2 vs. PC3) for 12 elements

Epithermal quartz-pyrite-stibnite-realgar-orpiment veins are the last stage of epithermal veining and are characterized an increasing As and/or Sb-bearing minerals, pyrite, arsenopyrite, and locally cinnabar. These veins host the main zone of gold mineralization (Richards et al., 2006; Niroomand et al., 2013). The veins containing quartz-calcite-pyrite-Galena±sphalerite with higher Ag concentrations mainly occur outside the main gold mineralization zone in propylitic alteration areas (Rastad et al., 2000; Richards et al. 2006). Thus, the two sub-clusters are separated from each other.

The Co-Ti-Cr-Ni-V-Fe is observed as a separate group, which implies a different origin. It also shows two sub-groups Co-Ti-Cr-Ni, and Fe-V. The abundance of magnetite, hematite, limonite, and minerals such as rutile and ferromagnesian minerals in host rocks can be the second group's main sources. Magnetite is associated with quartz-sulfide-magnetite veins, and hematite and limonite are enriched in the supergene alteration zone (Richards et al., 2006; Niroomand et al., 2013).

Besides, source identification can be obtained from the PCA. High loading of Co-Ti-Cr-Ni-V-Fe in the first component confirms the results of CA, suggesting a common source. The second component, including As-Sb-Hg-S-Pb, shows a strong correlation. A high loading is observed between Fe and Zn in the third group (PC3), but no positive correlation is seen in Pearson's correlation; thus, they have no common source.

Some elements show an affinity for more than one geochemical group. For example, iron is a siderophile, but it acts as a chalcophile and lithophile element in the earth`s crust (Mason & Moore, 1982). It seems Fe has a relatively high loading in the first and third components, suggesting it may have distinct origins: silicate and oxide minerals as well as sulfides (pyrite).

Conclusion

This investigation was conducted to determine the concentrations, contamination, and source of some heavy metals and metalloids in soil samples around the Sari Gunay gold mine, Kurdistan Province, west Iran. The results indicate that the distribution of As, Sb, Co, Cr, Hg, Pb, Zn, Ni, V, and Ti in the soils is not uniform over the study area. Their concentrations change according to distance from the mine and mineral processing plant.

Based on CF and EF indices, soil samples show extremely high to high contamination of Hg, Sb, As, and Pb. The order of mean CF is Hg > Sb > As > Pb > Zn > V > Ti > Ni > Cr > Co, and mean EF is also the same as CF values. The high contamination degree of the Hg, Sb, As, and Pb is related to gold mineralization and its paragenesis minerals such as cinnabar, stibnite, realgar, orpiment, and galena. The calculated CF and EF are uncontaminated or moderately contaminated for Zn, V, Ti, Cr, and Co.

The correlation analysis, PCA, and CA analyses were used to find insight into the sources of metals and metalloids in soil samples. Relationships between elements concentration in the soil samples indicated Hg, As, Sb, Pb, and S are positively correlated, showing the same origin of these metals. Titanium, V, Ni, Cr, Co, and Fe are also distinguished to have the same source. Two main sources for the studied elements were identified. Mercury, As, Sb, Pb, and Zn are attributed to sulfide mineralization, which originates mainly from both geogenic and anthropogenic sources. Furthermore, Ti, V, Ni, Cr, Co, and Fe originate mainly from geogenic sources, including supergene alteration zone and silicate minerals in host rocks.

Acknowledgement

The authors wish to thank Bu-Ali Sina University, Hamedan, Iran, for financial support. The authors would also like to thank two anonymous reviewers who helped improve this paper.

References

Abdul-Wahab, S.A., Marikar, F.A., 2012. The environmental impact of gold mines: pollution by heavy metals. Central European Journal of Engineering, 2(2): 304-313.

Abiya S.E., Odiyi, B.O., Ologundudu, F.A., Akinnifesi, O.J., Akadiri, S., 2019. Assessment of Heavy Metal Pollution in a Gold Mining Site in Southwestern Nigeria. Biomedical Journal of Scientific & Technical Research, 12(4): 9353-9357.

Acosta, J.A., Faz, A., Martinez, M., Zornoza, R., Carmona, D.M., Kabas, S., 2011. Multivariate statistical and GIS-based approach to evaluate heavy metals behavior in mine sites for future reclamation. Journal of Geochemical Exploration, 109(1-3): 8-17.

Adewumi, A.J., Laniyan, T.A., 2020. Contamination, sources and risk assessments of metals in media from Anka artisanal gold mining area, Northwest Nigeria. Science of the Total Environment, 718: 137235.

Adriano, D.C., 1986. Trace elements in the terrestrial environment. Springer -Verlag, New York, 867 p.

Armah, F.A., Quansah, R., Luginaah, I.A., 2014. Systematic Review of Heavy Metals of Anthropogenic Origin in Environmental Media and Biota in the Context of Gold Mining in Ghana. International Scholarly Research Notices, 37.

Bolourchi, M.H., 1979. Explanatory text of the Kabudar Ahang Map, Geological Survey of Iran No. D5, scale l/250000.

Caeiro, S., Costa, M.H., Ramos, T.B., Fernandes, F., Silveira, N., Coimbra, A., Medeiros, G., Painho, M., 2005. Assessing heavy metal contamination in Sado Estuary sediment. An index analysis approach. Ecological Indicators, 5: 151-169.

Carver, R.E., 1971. Procedures in sedimentary petrology. John Wiley & Sons, 653 p.

Demková1, L., Jezný, T., Bobuľská, L., 2017. Assessment of Soil Heavy Metal Pollution in a Former Mining Area - Before and After the End of Mining Activities. Soil and Water Research, 12(4): 229-236.

Donkor, A.K., Bonzongo, J.C.J., Nartey, V.K., Adotey, D.K., 2005. Heavy metals in sediments of the gold mining impacted Pra River basin, Ghana, West Africa. Soil and Sediment Contamination, 14(6): 479-503.

Dragovıć, S., Mihailovıć, N., Gajıć, B., 2008. Heavy metals in soils: distribution, relationship with soil characteristics and radionuclide's and multivariate assessment of contamination sources. Chemosphere, 72(3): 491-549.

Ebenebe, P., Shale, K., Sedibe M.M., Achilonu, M., Tikilili, P.V., 2017. South African Mine Effluents: Heavy Metal Pollution and Impact on the Ecosystem. International Journal of Chemical Sciences, 15(4): 198.

Folk, R.L., 1974. Petrology of Sedimentary Rocks. Hemphill Publishing Co., Austin, 170 p.

Fuge, R., Paveley, C.F., Holdham, M.T., 1989. Heavy metal contamination in the Tanat Valley, North Wales. Environmental Geochemistry and Health, 11: 127-135.

Gafur, N.A., Masayuki, S., Sakae, S., Koichiro, S., 2018. A Case Study of Heavy Metal Pollution in Water of Bone River by Artisanal Small-Scale Gold Mine Activities in Eastern Part of Gorontalo, Indonesia. Water, 10(11): 1507.

Gholizadeh, A., Borůvka, L., Seberioon, M.M., Kozák, J., Vašát, R., Němeček, K., 2015. Comparing different data pre-processing methods for monitoring soil heavy metals based on soil spectral features. Soil and Water Research, 10: 218-227.

Gzik, A., Kuehling, M., Schneider, I., Tschochner, B., 2003. Heavy metal contamination of soils in a mining area in South Africa and its impact on some biotic systems. Journal of Soils and Sediments, 3(1): 29-34.

Håkanson, L., 1980. An ecological risk index for aquatic pollution control. A sedimentological approach. Water Research, 14: 975-1001.

Hernandez, L., Probst, A., Probst, J.L., Ulrich, E., 2003. Heavy metal distribution in some French forest soils: evidence for atmospheric contamination. Science of the Total Environment, 312: 195-219.

Hou, D., He, J., Lu, C., Ren, L., Fan, Q., Wang, J., Xie, Z., 2013. Distribution characteristics and potential ecological risk assessment of heavy metals (Cu, Pb, Zn, Cd) in water and sediments from Lake Dalinouer, China. Ecotoxicology and Environmental Safety, 93: 135-144.

Johnbull, O., Abbassi, B., Zytner, R.G., 2019. Risk assessment of heavy metals in soil based on the geographic information System-Kriging technique in Anka, Nigeria. Environmental Engineering Research, 24(1): 150-158.

Jung, M.C., 1995. Heavy Metal Contamination of Soils, Plants, Waters and Sediments in the Vicinity of Metalliferous Mines in Korea. Ph.D. thesis, University of London.

Jung, M.C., Thornton, I., 1997. Environmental contamination and seasonal variation of metals in soils, plants and waters in the paddy fields around a Pb-Zn mine in Korea. Science of the Total Environment, 198: 105-121.

Kabata-Pendias, A., 2011. Trace elements in soils and plants, 4th ed. CRC Press, Taylor and Francis Group Press, New York, 432 p.

Karn, R., Ojha, N., Abbas, S., Bhugra, S., 2021. A review on heavy metal contamination at mining sites and remedial techniques. IOP Conference Series: Earth and Environmental Science, 796: 012013.

Khan Nazer, N.H., 2015. Geological map of the Kohin Quadrangle. Geological Survey of Iran, Geological Quadrangle Map No. 5660, scale l/100000.

Khosravi, M., Saadat, S., Dabiri, R., 2020. Evaluation of heavy metal contamination in soil and water resources around Taknar copper mine (NE Iran). Iranian Journal of Earth Sciences, 12(3): 212-222.

Lewis, D.W., McConchie, D., 1994. Analytical Sedimentology. Springer, 197 p.

Liang, Y., Yi, X., Dang, Z., Wang, Q., Luo, H., Tang, J., 2017. Heavy metal contamination and health risk assessment in the vicinity of a tailing pond in Guangdong, China. International journal of environmental research and public health, 14(12): 1557.

Lizárraga-Mendiola, L., González-Sandoval, M.R., Durán-Domínguez, M.C., Márquez-Herrera C., 2009. Geochemical behaviour of heavy metals in a Zn-Pb-Cu mining area in the State of Mexico (central Mexico). Environmental Monitoring and Assessment, 155: 355-372.

Loska, K., Wiechuya, D., 2003. Application of principal component analysis for the estimation of source of heavy metal contamination in surface sediments from the Rybnik Reservoir. Chemosphere, 51: 723- 733.

Mandeng, E.P.B., Bidjeck, L.M.B., Bessa, A.Z.E., Ntomb, Y.D., Wadjou, J.W., Doumo, E.P.E.,

Dieudonn, L.B., 2019. Contamination and risk assessment of heavy metals, and uranium of sediments in two watersheds in Abiete-Toko gold district, Southern Cameroon. Heliyon, 5: e02591.
Mason, B.H., Moore, C.B., 1982. Principles of geochemistry. John Wiley & Sons, 344 p.
Mehrabi, B., Mehrabani, Sh., Rafiei, B., Yaghoubi, B., 2015. Assessment of metal contamination in groundwater and soils in the Ahangaran mining district, west of Iran. Environmental Monitoring and Assessment, 187: 727.
Merrington, G., Alloway, B.J., 1994. The transfer and fate of Cd, Cu, Pb and Zn from historic metalliferous mine sites in the UK. Applied Geochemistry, 9: 677-687.
Mishra, V.K., Kim, K.H., Kang, C.H., Choi, K.C., 2004. Wintertime sources and distribution of airborne lead in Korea. Atmospheric Environment, 38(17): 2653-2664.
Niroomand, S., Rastad, E., Rashidnejad-Omran, N., Ghaderi, M., 2013. Geology and mineralization of the Dashkasan (Sari Gunay) epithermal gold deposit, Sanandaj-Sirjan zone, east of Qorveh, Kordestan Province. Geoscience, 22 (88.3): 30-41.
Okereafor, U., Makhatha, E., Mekuto, L., Mavumengwana, V., 2019. Dataset on assessment of pollution level of selected trace metals in farming area within the proximity of a gold mine dump, Ekuhurleni, South Africa. Data in brief, 26: 104473.
Percival, J.B., White, H.P., Goodwin, T.A., Parsons, M.B., Smith, P.K., 2014. Mineralogy and spectral reflectance of soils and tailings from historical gold mines, Nova Scotia. Geochemistry: Exploration, Environment, Analysis, 14(1): 3-16.
Rafie, B., Ahmadi-Ghomi, F., Karimkhani, A., 2017. Assessment of the anthropogenic influx of metallic pollutants in the Sefidrud delta, Gilan Province, Iran. Marine Pollution Bulletin, 121: 381-389.
Rafiei, B., Bakhtiari Nejad, M., Hashemi, M., Khodaei, A.S., 2010a. Distribution of heavy metals around the Dashkasan Au mine. International Journal of Environmental Research, 4(4): 647-654.
Rafiei, B., Khodaei, A. Khodabakhsh, S. Hashemi, M., Bakhtiari Nejad, M., 2010b. Contamination assessment of lead, zinc, copper, cadmium, arsenic and antimony in Ahangaran mine soils, Malayer, West of Iran. Soil and Sediment Contamination An International Journal, 19 (5): 573-586.
Ranjbarian, S., 2018. Study of mineralogy and geochemistry of sulphide minerals in Sari Gunay gold deposit (NE Qorveh). M.Sc. thesis, Bu-Ali Sina University.
Rastad, E., Niroomand, S., Hashem-Emami, M., Rashidnejad-Omran, N., 2000. Genesis of Sb-As-Au deposit in Volcano-Plutonic Complex of Dashkasan (east Qorveh, kordestan Province). Geoscience, 9(37-38): 2-23.
Richards, J.P., Wilkinson, D., Ullrich, T., 2006. Geology of the Sari Gunay Epithermal Gold Deposit, Northwest Iran. Economic Geology, 101(8): 1455-1496.
Rudnick, R.L., Gao, S., 2003. Composition of the continental crust. In: Rudnick, R.L., Holland, H.D., Turekian, K.K. (Eds.), Treatise on geochemistry- The Crust. Elsevier, Oxford, pp. 1-64.
Ruilian, Y., Xing, Y., Yuanhui, Z., Gongren, H., Xianglin, T., 2008. Heavy metal pollution in intertidal sediments from Quanzhou Bay, China. Journal of Environmental Sciences, 20: 664-669.
Segura, r., Arancibia, V., Zuniga, M.C., Pasten, P., 2006. Distribution of copper, zinc, lead and cadmium concentrations in stream sediments from the Mapocho River in Santiago, Chile. Journal of Geochemical Exploration, 91: 71-80.
Stöcklin, J., 1968. Structural history and tectonic of Iran; a review. American Association of Petroleum Geologists Bulletin, 52: 1229-1258.
Straskraba, V., Moran, R.E., 1990. Environmental occurrence and impacts of arsenic at gold mining sites in the western United States. International journal of mine water, 9(1): 181-191.
Sutherland, R.A., 2000. Bed sediment-associated trace metals in an urban stream, Oahu, Hawaii. Environmental Geology, 39: 611-627.
Sutherland, R.A., Tolosa, C.A., Tack, F.M.G., Verloo, M.G., 2000. Characterization of selected element concentrations and enrichment ratios in background and anthropogenically impacted roadside areas. Archives of Environmental Contamination and Toxicology, 38: 428-438.
Tomlinson, D.L., Wilson, J.G., Harris, C.R., Jeffrey, D.W., 1980. Problems in the assessment of heavy-metal levels in estuaries and the formation of a pollution index. Helgoländer Meeresuntersuchungen, 33: 566-575.
Wang, X., He, M., Xie, J., Xi, J., Lu, X., 2010. Heavy metal pollution of the world largest antimony mine-affected agricultural soils in Hunan province (China). Journal of Soils and Sediments, 10: 827-837.

Xiao, R., Wangc, S., Ronghua, L., Wang, J.J., Zhanga, Z., 2017. Soil heavy metal contamination and health risks associated with artisanal gold mining in Tongguan, Shaanxi, China. Ecotoxicology and Environmental Safety, 141: 17-24.

Yongming, H., Peixuan, D., Junji, C., Posmentier, E.S., 2006. Multivariate analysis of heavy metal contamination in urban dusts of Xi'an, Central China. Science of the Total Environment, 355: 176-186.